2.

Conf-920748--4

Received OSTI

AUG 17 1992

PNL-SA--21162

DE92 019356

ALTERNATIVE MATERIALS FOR SOLID OXIDE FUEL CELLS: FACTORS AFFECTING AIR-SINTERING OF CHROMITE INTERCONNECTIONS

L. A. Chick
J. L. Bates

July 1992

Presented at the
DOE 4th Annual Fuel Cells Contractors
Review Meeting
July 14-15, 1992
Morgantown, West Virginia

Work supported by
the U.S. Department of Energy
under Contract DE-AC06-76RLO 1830

Pacific Northwest Laboratory
Richland, Washington 99352

MASTER

DISTRIBUTION OF THIS DOCUMENT IS UNLIMITED

DISCLAIMER

This report was prepared as an account of work sponsored by an agency of the United States Government. Neither the United States Government nor any agency thereof, nor any of their employees, makes any warranty, express or implied, or assumes any legal liability or responsibility for the accuracy, completeness, or usefulness of any information, apparatus, product, or process disclosed, or represents that its use would not infringe privately owned rights. Reference herein to any specific commercial product, process, or service by trade name, trademark, manufacturer, or otherwise does not necessarily constitute or imply its endorsement, recommendation, or favoring by the United States Government or any agency thereof. The views and opinions of authors expressed herein do not necessarily state or reflect those of the United States Government or any agency thereof.

Alternative Materials for Solid Oxide Fuel Cells: Factors Affecting Air-Sintering of Chromite Interconnections

CONTRACT INFORMATION

Contract Number (FTPA)	13822
Contractor	Pacific Northwest Laboratory Operated for the U.S. Department of Energy by Battelle Memorial Institute under contract DE-AC06-76RLO 1830 P. O. Box 999 Richland, Washington 99352 (509) 375-2579
Contractor Project Manager	Dr. J. Lambert Bates
Principal Investigators	Dr. Larry A. Chick Dr. J. Lambert Bates
METC Project Manager	William Huber/Diane Hooie
Period of Performance	April 1, 1991 to June, 1991

Schedule and Milestones

FY92 Program Schedule

	S O N D J F M A M J J A S
Materials Development and Property Evaluation	----------
Materials Synthesis	----------
Materials Processing and Fabrication	----------
Electrochemical Processes	----------

OBJECTIVES

The purpose of this research is to develop alternative materials for solid oxide fuel cell (SOFC) interconnections and electrodes with improved electrical, thermal and electrochemical properties. Another objective is to develop synthesis and fabrication processes for these materials whereby they can be consolidated in air into SOFCs. The approach is to (1) develop modifications of the current, state-of-the-art materials used in SOFCs, (2) minimize the number of cations used in the SOFC materials to reduce potential deleterious interactions, (3) improve thermal, electrical, and electrochemical properties, (4) develop methods to synthesize both state-of-the-art and alternative materials for the simultaneous fabrication and consolidation in air of the interconnections and electrodes with the solid electrolyte, and (5) understand electrochemical reactions at materials interfaces and the effects of component compositions and processing on those reactions.

BACKGROUND

Solid oxide fuel cells (SOFCs) continue to develop as promising, clean, and efficient technology for the direct conversion of hydrogen and fossil fuels to electrical energy. State-of-the-art concepts generally use the same materials as the air electrodes, La(Sr)MnO_3 (sometimes containing stabilized-ZrO_2 particles); the fuel electrode, ZrO_2/Ni composite; the interconnection, La(Mg)CrO_3 or La(Sr)CrO_3, and the electrolyte, Y_2O_3-stabilized ZrO_2. The use of these different material combinations of manganite, chromite, zirconia, and Ni in state-of-the-art SOFCs pose several materials fabrication and performance-related problems.

New alternative materials with improved properties that can be more easily fabricated into fuel cells are needed for the further development of SOFC with lower costs and improved performance. An important key is the development of an SOFC interconnection material that can be sintered in air to a high density at temperatures <1550°C. It should have a good thermal expansion match with and intimately bond to both the air and fuel electrodes, without forming deleterious interaction products at the interfaces. At the present time this has not been attained with the state-of-the-art $La_{1-x}Sr_xCrO_3$ interconnections.

PROJECT DESCRIPTION

The overall approach for this research and development is to:

- Minimize the number of cations in the electrode-electrolyte-interconnection by developing yttrium compounds, such as Y(Ca)CrO_3 as the interconnection, and Y(M')MnO_3 as the air electrode.

- Develop advanced synthesis and fabrication processes for air sintering below 1550°C of chromite interconnections through (1) the use of sintering aids; and (2) the synthesis of submicrometer, active powders.

- Establish methods for the simultaneous processing and consolidation of air-sinterable powders.

- Develop complex La(M')[Cr,M"]O_3 or Y(M')(Cr,M")CrO_3 compounds with modified thermal expansion and electrical conductivity.

- Electrochemically evaluate interface reactions (in reproducible and controlled laboratory tests) for both the alternative and state-of-the-art materials and cell components developed under this program.

This paper describes a comprehensive study that assessed the effects of composition, time and temperature on the air sintering of three chromite systems. Systems studied were $Y_{0.7}Ca_xCrO_3$ (YCC), $La_{0.7}Ca_xCrO_3$ (LCC), and $La_{0.7}Sr_xCrO_3$ (LSC). The effects on sintering of additives to the B-site, as partial substitutions for Cr, were also assessed.

RESULTS

Experimental Procedures

Chromite powders were synthesized by the glycine/nitrate process using a "stoichiometric" molar ratio of glycine-to-nitrate (g/n≈0.55)[1,2,3]. The powder was calcined at 650°C for 0.5 hr, uniaxially pressed (no binder) at 35 MPa and then isostatically pressed at 140 MPa into appx. 21 mm diameter by 3 mm thick samples. The pellets were set on edge in alumina racks and sintered in an electrical resistance-heated furnace in air. Sintered densities were determined by immersion weighing in ethyl alcohol. Theoretical densities were calculated from lattice parameters determined by X-ray diffraction on the perovskite phase. Theoretical densities used were: 5.35 g/cm^3 for $Y_{0.7}Ca_xCrO_3$, 6.07 g/cm^3 for $La_{0.7}Ca_xCrO_3$, and 6.41 g/cm^3 for $La_{0.7}Sr_xCrO_3$ (x nominally 0.3).

Effect of A/B Cation Ratio

Previous studies have demonstrated that slight enrichment or depletion of the "A-site" cations in relation to the "B-site" cation (Cr) can substantially alter sintering behavior of the ABO_3-type-perovskite chromites[4,5]. In order to allow a direct comparison to data published by Mori et al[6], the same substitution scheme was adopted in the present study; that is, the A/B site ratio was altered by depleting or enriching the rare earth substitution cation with the La or Y and the Cr concentrations held constant: (La or $Y)_{0.7}$(Ca or Sr)$_xCrO_3$. In this scheme, rare earth depletion is achieved when x<0.3, and enrichment occurs when x>0.3. Mori and coworkers reported data for $La_{0.7}Ca_xCrO_3$ with x=0.30 and 0.32. However, due to the difficulty of replicating chromite compositions to the necessary high accuracy using different synthesis techniques, compositions with a range of rare earth levels were prepared and sintered, using the sintering behavior as the indicator of relative compositions. In effect, sintered density was used as the analytical chemistry technique. Samples were prepared in each chromite system with x= 0.28, 0.29, 0.30, 0.31, and 0.32, with a *relative precision* of ±0.001 or better. Samples were heated at 100°C/hr to 1400°C, then air quenched. A comparison of the data from the current study to that reported by Mori et al is shown in Figure 1. The samples with x=0.32 behave similarly, but the sintered density of the Mori et al sample with x=0.30 was substantially lower and may actually have been comparable to a PNL composition with x≈0.295. However, the *trends* in the data are similar with a substantial *increase* in sintered density as calcium content is increased between x=0.29 and 0.32. This comparison reinforces the need to examine sintering effects in chromites over a range of A/B ratios rather than performing experiments at single A/B ratios, due to the difficulty of accurately controlling chromite compositions.

Figure 2 compares data from Mori et al to that of the present study for $La_{0.7}Ca_{0.32}CrO_3$ samples heated to various temperatures and quenched. The curves cross at 1200°C with the PNL samples showing higher sintered densities at higher temperatures. Because of differences in powder synthesis techniques, it is likely that the PNL samples had lower green densities, resulting from smaller particle size. The PNL powders, being more active, would be expected to shrink more rapidly at lower temperatures than would the Mori samples. In addition, as discussed elsewhere[4], variations in synthesis

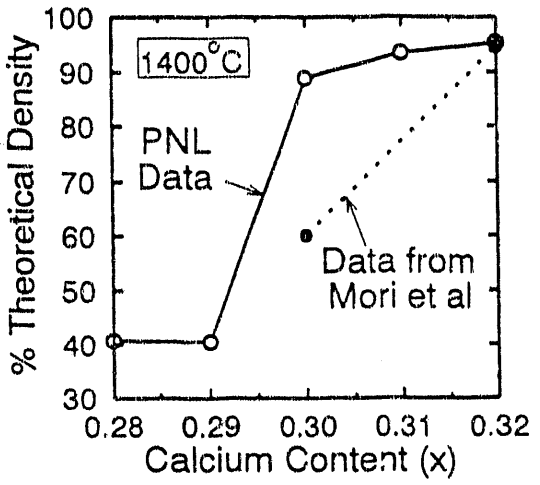

Figure 1. Percent of theoretical density achieved is plotted versus calcium content for $La_{0.7}Ca_xCrO_3$ samples heated to 1400°C at 100°/hr and air quenched. Mori et al data from reference 6.

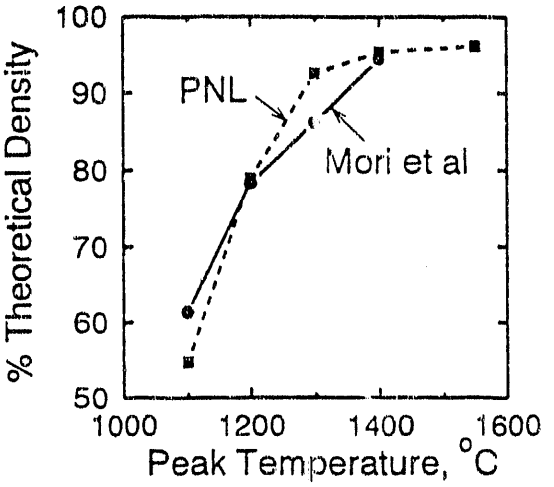

Figure 2. Percent of theoretical density achieved is plotted versus peak sintering temperature for $La_{0.7}Ca_{0.32}CrO_3$ samples heated at 100°/hr and air quenched.

procedure may result in differing amounts of chromate phase exsolution, causing later differences in the extent of liquid-phase sintering.

The effects of A/B ratio and peak temperature for the three chromite systems are illustrated in Figures 3, 4 and 5. These chromites were heated at 100°C/hr to the peak temperature and air quenched. The trend seen in Figure 1 for the LCC system at 1400°C also holds for LCC samples sintered to the other peak temperatures (Figure 3). At temperatures as low as 1100°C, the A/B ratio has a substantial effect on sintered density.

In the LSC system, Figure 4, the highest densities are achieved for the highest strontium enrichment, x=0.32. However a local minimum is observed for x=0.31 at 1300°C and above. A similar local minimum was observed for LSC in a previous study[4] although that study used a different substitution scheme and the chromites were sintered at 1550°C for 8 hr, resulting in the minima occurring for the stoichiometric composition (A/B=1.0).

In the YCC system, Figure 5, the sintered density is only slightly affected by changes in A/B ratio, although sintered densities generally increase slightly with increasing calcium content. The previous study[4] found a much larger A/B ratio affect on sintering in the YCC system, and this also could be attributed to the different substitution scheme and sintering schedule.

Long-Term Sintering

Based on the results shown in Figures 3-5, two compositions were chosen from each chromite system to be sintered for longer times and at different temperatures. For each system, compositions were chosen with a separation of 0.02 in alkaline earth content, one composition relatively depleted in alkaline earth and the other relatively enriched. These compositions were then heated to a given temperature at 100°C/hr and then held for periods of from 8 to 168 hr. Results for sintering at 1200°, 1300°, and 1400°C are shown in Figures 6, 7 and 8, in

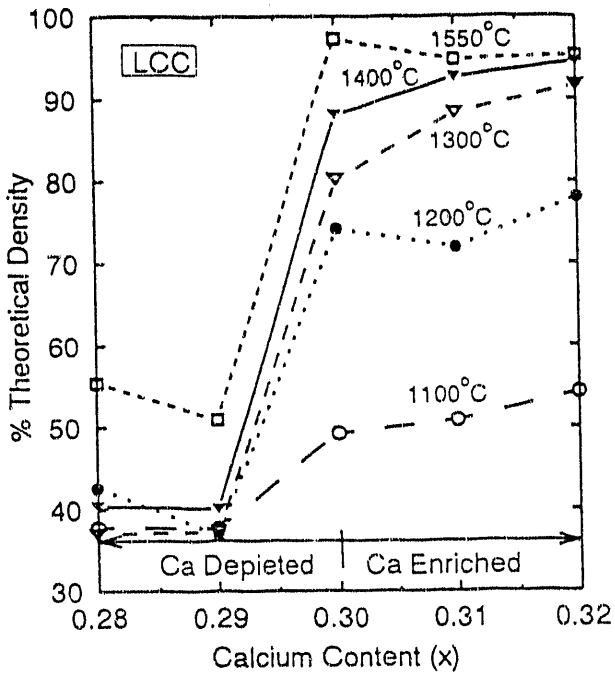

Figure 3. Percent of theoretical density achieved is plotted versus calcium content for $La_{0.7}Ca_xCrO_3$ samples heated to various peak temperatures at 100°/hr and air quenched.

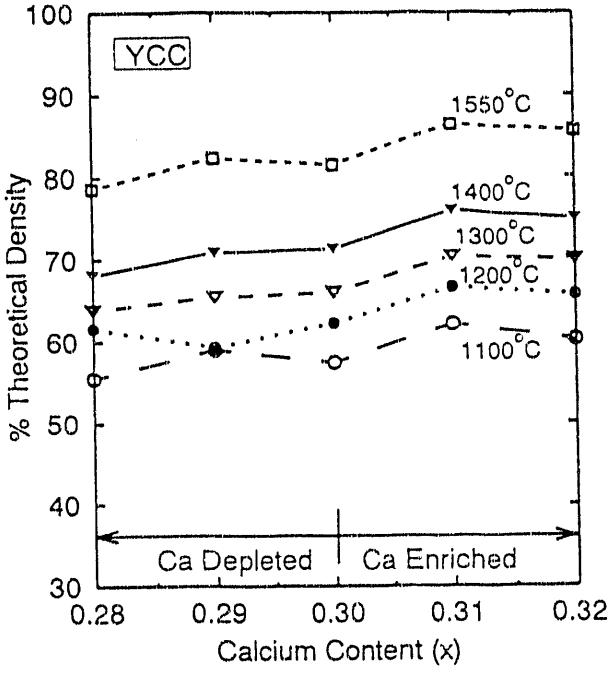

Figure 5. Percent of theoretical density achieved is plotted versus calcium content for $Y_{0.7}Ca_xCrO_3$ samples heated to various peak temperatures at 100°/hr and air quenched.

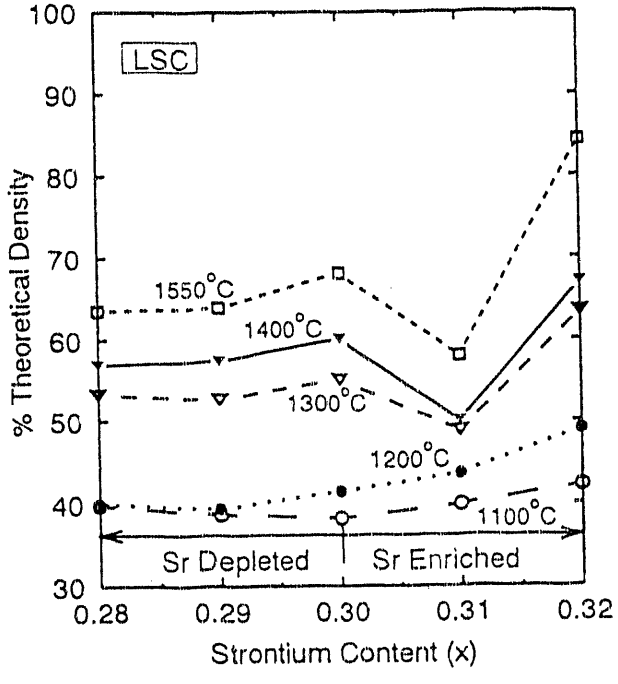

Figure 4. Percent of theoretical density achieved is plotted versus strontium content for $La_{0.7}Sr_xCrO_3$ samples heated to various peak temperatures at 100°/hr and air quenched.

which the time-zero data are taken from Figures 3-5.

In Figures 6-8, the *relative* sintering characteristics of the different chromites do not change except for the case of the longest time at 1400°C (Figure 8 at 168 hr). Under all other conditions, LCC29 and LCC31 have the lowest and highest sintered densities, respectively; the LSC and YCC compositions exhibit intermediate sintered densities, with LSC sintered densities always lower than those of YCC.

For all of the compositions, sintering rates decrease with time, as expected. Some compositions, notably LCC31 at all temperatures and LSC30 at 1200° and 1300°C, densities actually *decrease* at intermediate times. These apparently decreasing densities may be due to immersion weighing errors in those cases where relative densities are low. However, for LCC31, repetition of the density determinations and

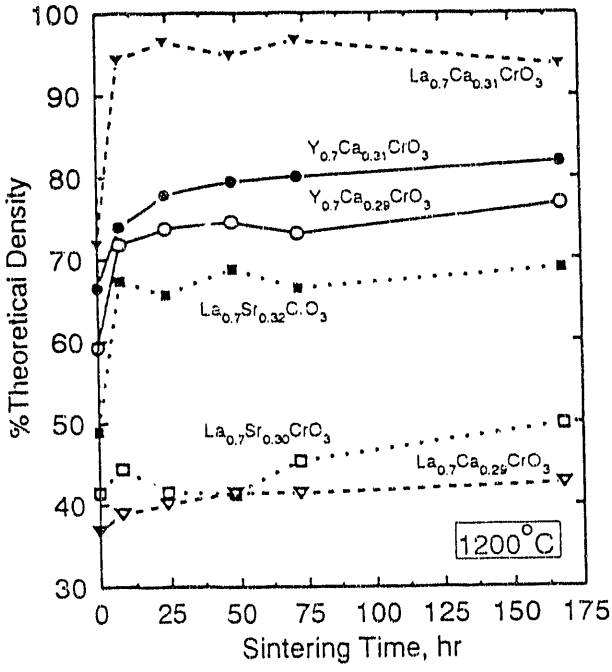

Figure 6. Percent of theoretical density achieved is plotted versus sintering time at 1200°C for six chromite compositions.

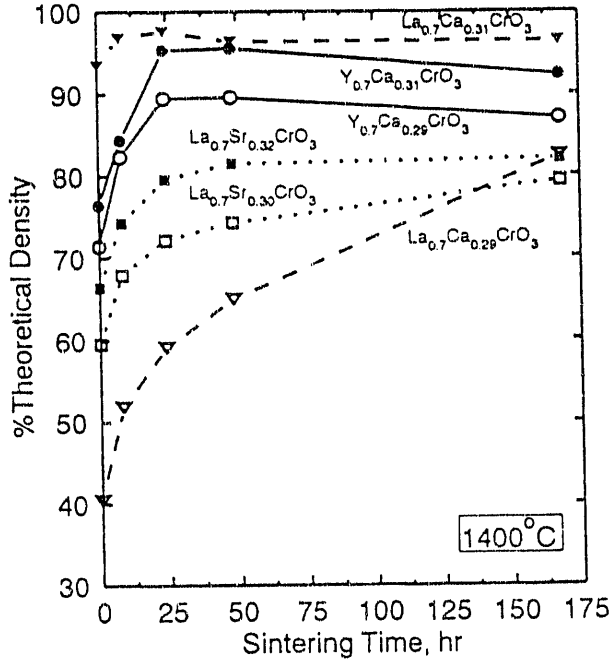

Figure 8. Percent of theoretical density achieved is plotted versus sintering time at 1400°C for six chromite compositions.

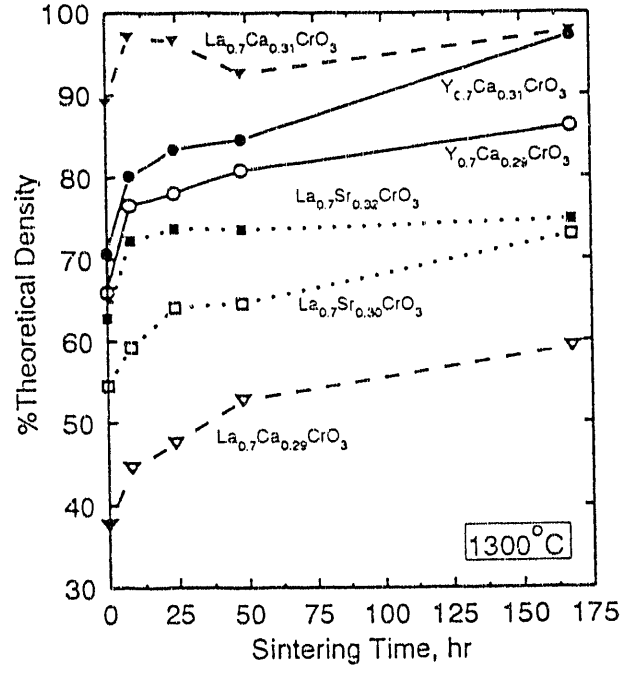

Figure 7. Percent of theoretical density achieved is plotted versus sintering time at 1300°C for six chromite compositions.

optical microscopy indicate that the effect is real. LCC31 attains maximum density between 8 and 24 hr. The causes of subsequent decreases in density of LCC31 are not understood, but may be related to oxygen deficiency, gradual phase changes, or slight bloating due to gas pressure inside closed pores.

Although the chromites that sinter to relatively high densities below 1400°C densify primarily via a liquid-phase mechanism (see below), LCC29 and LSC30 probably sinter via solid state transport at high temperatures *after experiencing low-temperature, transient liquid-phase sintering events.* Figure 9 is a log-log plot of linear shrinkage (calculated from sample densities) versus time for compositions sintered at 1400°C. The slope for LCC29 indicates approximately $t^{1/3}$ dependence, whereas that for LSC30 changes to $t^{1/5}$ dependence after 24 hr. The early-stage $t^{1/3}$ dependence may indicate a solid-state grain-boundary diffusion mechanism[7].

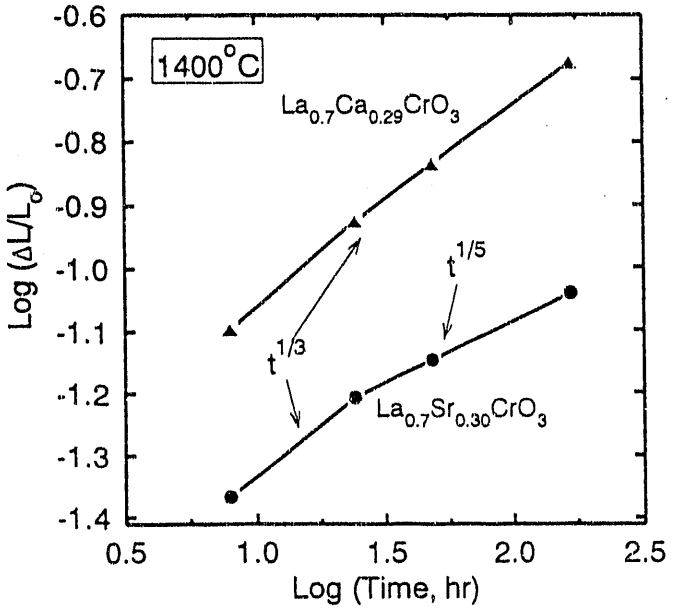

Figure 9. Logarithm of relative sintering shrinkage is plotted versus logarithm of sintering time at 1400°C for two chromite compositions.

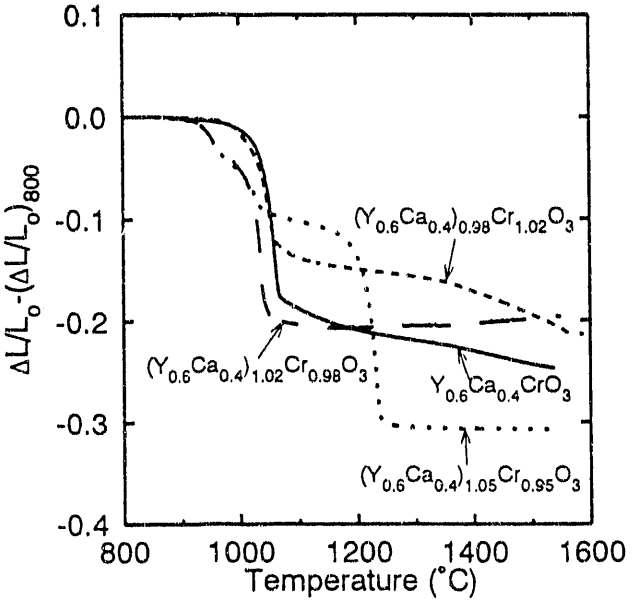

Figure 10. Sintering shrinkage is plotted versus temperature for $(Y_{0.6}Ca_{0.4})_{(1-y)}Cr_{(1+y)}O_3$ samples heated at 100°C/hr in a dilatometer.

Sintering Shrinkage Curves

The mechanisms of chromite sintering were investigated using dilatometry to monitor sample shrinkage at controlled heating rates. Previously[4] sintering shrinkage curves for $Y_{1-x}Ca_xCrO_3$, were used to demonstrate that increasing the calcium content (while holding A/B=1.0) increased the magnitude of a rapid-shrinkage event beginning near 1020°C. Dilatometry studies were subsequently performed on YCC compositions with varied A/B ratios and for two LCC compositions. Although the substitution schemes and heating rates were slightly different for the YCC and the LCC samples, these systems exhibit similar behavior. As shown in Figures 10 and 11, two rapid-shrinkage events can occur in both systems. The first event occurs in *all* samples, beginning at about 1020°C for compositions with A/B≤1.0, and at about 950°C for compositions with A/B≥1.0. The second event only occurs for two compositions that have A/B>1.0, beginning at about 1200°C for $(Y_{0.6}Ca_{0.4})_{1.05}Cr_{0.95}O_3$ and at about 1150°C for $La_{0.7}Ca_{0.29}CrO_3$. In summary, these results indicate that enrichment of the A-site has two effects on the sintering curve; 1) the onset of the first rapid-shrinkage event is lowered in temperature by about 70° to approximately 950°C, and 2) a rapid-shrinkage event occurs near 1200°C that is not observed in samples with A-site depletion.

X-ray diffraction (XRD) was performed on the LCC compositions whose shrinkage curves are shown in Figure 11. Pellets were heated at 100°C/hr to a peak temperature, then quenched and powdered for XRD. The secondary phase, $CaCrO_4$, forms, melts, and redissolves into the perovskite matrix by 1200°C in both LCC compositions. Unit cell volumes were used to determine the amount of Ca present within the perovskite at each temperature. The amount of

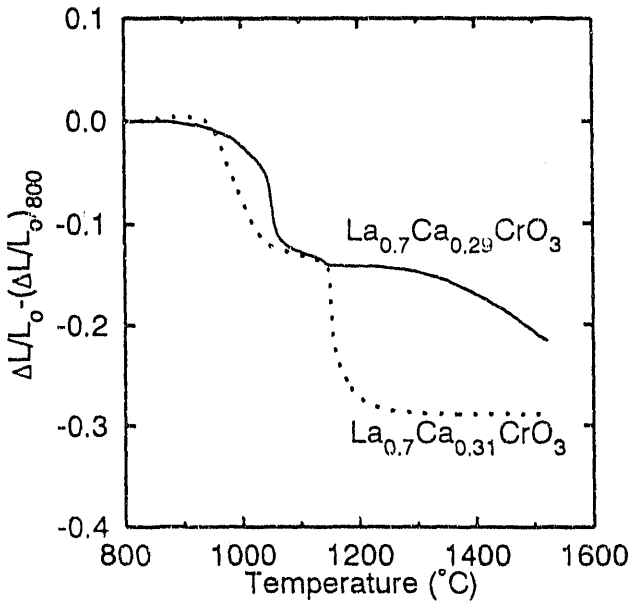

Figure 11. Sintering shrinkage is plotted versus temperature for $La_{0.7}Ca_xCrO_3$ samples heated at 100°C/hr in a dilatometer.

$CaCrO_4$ phase present was tracked by measuring peak intensities. Preliminary analysis of these data indicates that the rapid shrinkage events occur as the Ca *redissolves* into the perovskite. This redissolution occurs in *two stages* in the LCC31 material, whereas only one redissolution stage is observed in the LCC29 material.

Effects of B-site Substitution on Sintering of Chromites

One of the options for improving the sinterability of chromites in air is to utilize a sintering aid that does not cause harmful materials interactions. The first step in the search was to screen prospective additives to find those that increase sinterability. In order to assess the effects of substitution of various cations for Cr^{3+} on the B-site in $La(Sr)CrO_3$, several series of samples were prepared and sintered at 1550°C for 3 hours. Each series tested the effects of an additive on sintering of samples with various A/B site ratios. The samples had the general formula, $(La_{0.76}Sr_{0.24})_{(1-y)}(Cr_{0.9}M'_{0.1})_{(1+y)}O_3$, where M' is the B-site additive of interest in the series.

The effects of Al, Zn, Co and Cu are compared to a control with no B-site dopant, Figure 12. In general, the results show that these additives have relatively small effects on sintering when the A-site is enriched (A/B>1), but can have substantial effects when the B-site is enriched (A/B<1). These results clearly demonstrate that Al substitution is either neutral (A/B>1), or severely detrimental (A/B<1) to sintering of this chromite. On the other hand, Co is apparently beneficial for A/B≤1, while Cu and Zn are beneficial mainly when A/B<1.

Since it had been determined that additives have the greatest effects when A/B<1, several other species were tested at only two A/B values, 1.0 and 0.9. The results, plotted in Figure 13, show that Zr is extremely detrimental for both levels, while Ni, Ga, and Mg are beneficial at both levels. The additives, Ag, Mn, and Fe appear to benefit sintering slightly at A/B=0.9, but hinder sintering at A/B=1.

The addition of Co is shown to be more effective in the LSC system (A/B≤1) than in LCC or YCC, as shown in Figure 14. The explanation may be that addition of Co induces liquid phase formation in LSC when A/B=1 or greater. In contrast, substantial liquid phase already present in LCC and YCC, even without the addition of Co.

Conclusions

Sintering of chromites with varied cation ratios showed that at temperatures as low as 1100°C, the A-site/B-site ratio has a substantial effect on sintered density of $La_{0.7}Ca_xCrO_3$. For temperatures of 1200°, 1300°, and 1400°C, and times up to 48 hr, LCC29 and LCC31 have the

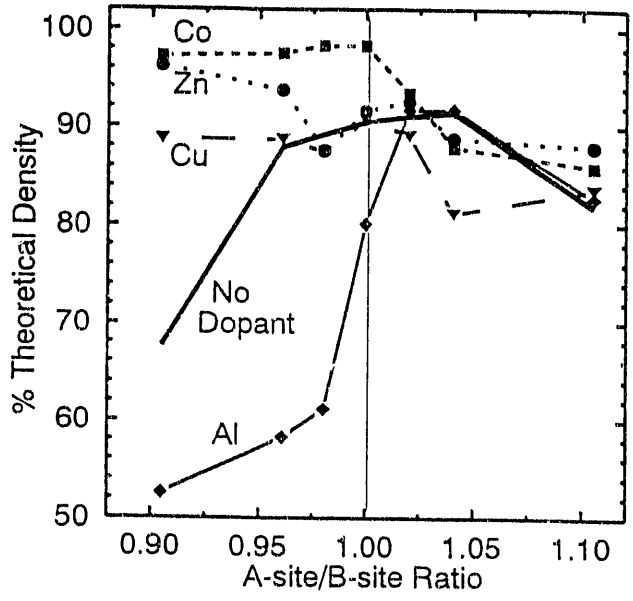

Figure 12. Sintered density is plotted versus A/B site ratio for $(La_{0.76}Sr_{0.24})_{(1-y)}(Cr_{0.9}M'_{0.1})_{(1+y)}O_3$, where M' is Co, Zn, Cu, or Al. Sintering was at 1550°C for 8 hr.

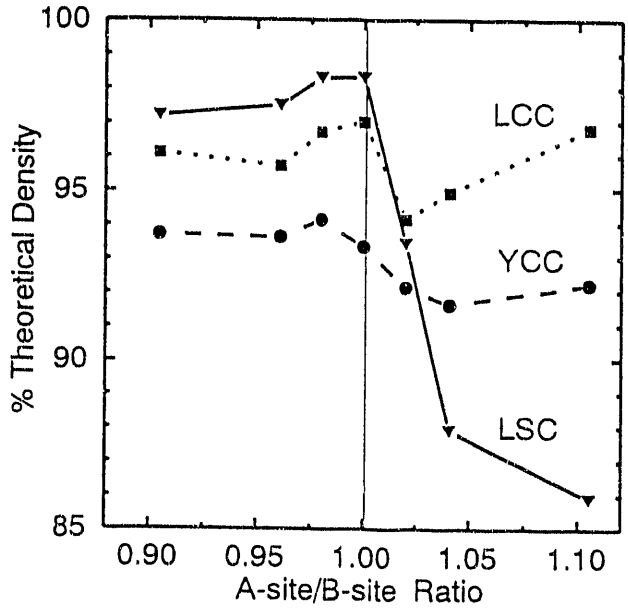

Figure 14. Sintered density is plotted versus A/B site ratio for $(LA_{0.7}RE_{0.3})_{(1-y)}(Cr_{0.9}Co_{0.1})_{(1+y)}O_3$, where LA is La or Y and RE is Sr or Ca. Sintering was at 1550°C for 8 hr.

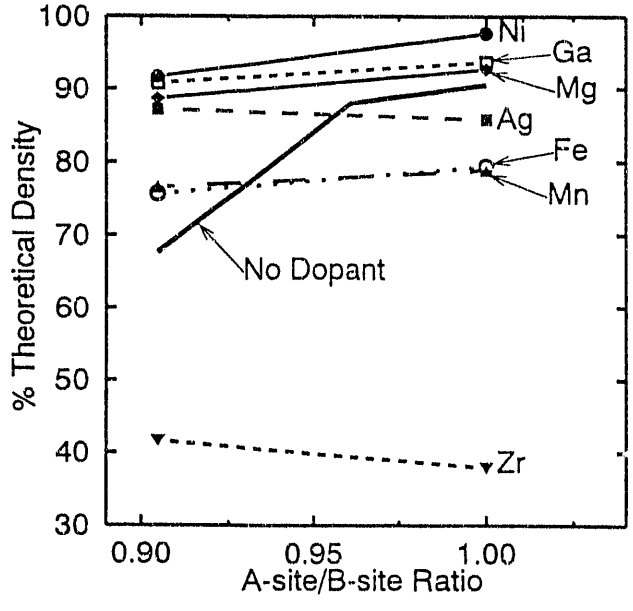

Figure 13. Sintered density is plotted versus A/B site ratio for $(La_{0.76}Sr_{0.24})_{(1-y)}(Cr_{0.9}M'_{0.1})_{(1+y)}O_3$, where M' is Ni, Ga, Mg, Ag, Mn, Fe, or Zr. Sintering was at 1550°C for 8 hr.

lowest and highest sintered densities, respectively; the LSC and YCC compositions exhibit intermediate sintered densities, with LSC sintered densities always lower than those of YCC. The chromites that sinter to relatively high densities at below 1400°C densify primarily via a liquid-phase mechanism, involving the exsolution, melting and subsequent redissolution of $CaCrO_4$.

Studies of additions to the B-site in chromites indicate that these additives have relatively small effects on sintering when the A-site is enriched, but can have substantial effects when the B-site is enriched. Al substitution is either neutral (A/B>1) or severely detrimental (A/B<1) to sintering of LSC. On the other hand, Co is beneficial for A/B≤1 while Cu and Zn are beneficial mainly when A/B<1. Zr is extremely detrimental for sintering of LSC, while Ni, Ga, and Mg are beneficial. The additives, Ag, Mn, and Fe appear to have only

slight effects. The addition of Co is more effective in the LSC system than in LCC or YCC.

Acknowledgements

The authors would like to thank GD Maupin, DE McCready, MJ Etchemendy, JA Baumann, and JL Aurand for technical assistance.

FUTURE WORK

The emphasis of this project over the next few years will shift from properties of individual SOFC materials to co-sintering and interactions between SOFC materials, including both state-of-the-art and alternative compositions. Compositions that are of particular interest are those that have been shown to have acceptable chemical, thermal and electrical properties **as individual materials** to warrant further development in combination with other candidate SOFC component compositions. Based on presently available data, viable candidates for interconnection include the state-of-the-art material, $La(Sr)CrO_3$, as well as two advanced alternatives, $Y(Ca)CrO_3$ and $La(Ca)CrO_3$. The corresponding manganites that are viable candidates for the air electrode, are $La(Sr)MnO_3$, $Y(Ca)MnO_3$, and $La(Ca)MnO_3$. Minor additives and/or adjustment of the cation ratios may be beneficial for improvement of the thermal expansion, sintering, and electrical transport in these materials.

Issues involved in co-sintering and interactions between couples of these materials and with the YSZ electrolyte will be investigated with emphasis on thermal expansion and sintering shrinkage tolerances for the sintering of thin-layer composites fabricated by colloidal processing techniques, diffusion of additive cations and wicking of transient liquid phases into adjacent components, formation of deleterious crystalline interaction phases between components, and effects of additives to interfaces between components.

In addition to interactions between components that occur during fabrication and sintering, this program will address mechanisms and effects of interactions that occur during SOFC operation. One of the goals of this work will be to develop valid accelerated testing techniques to predict the long-term performance of SOFC components and interfaces.

The simultaneous fabrication of these alternative, air-sinterable interconnection and air electrode materials with the electrolyte is a major direction of the program. These efforts will be integrated with the experiences, activities, and needs through cooperation with the other DOE and GRI solid oxide fuel cell contractors. Both data and materials will be made available for cooperative evaluation and testing.

REFERENCES

1. LA Chick, LR Pederson, GD Maupin, JL Bates, LE Thomas, and GJ Exarhos. "Glycine-Nitrate Combustion Synthesis of Oxide Ceramic Powders", Mater. Lett. 10 (1990) 6.

2. LA Chick, LR Pederson, GD Maupin and JL Bates. "Ultra-Fine Powders Using Glycine-Nitrate Combustion Synthesis", in Proceedings of the Fifth Annual Conference on Fossil Energy Materials. CONF-9105184 and ORNL/FMP-91/1 Oak Ridge National Laboratory, Oak Ridge, TN (1991) 117.

3. LA Chick, JL Bates, LR Pederson and HE Kissinger. "Synthesis of Air-Sinterable Lanthanum Chromite Powders", in Proceedings First International Symposium on Solid Oxide Fuel Cells. S.C. Singhal Ed. The Electrochemical Society, Pennington, NJ. (1989), 120.

4. LA Chick, JL Bates and GD Maupin. "Air-Sintering Mechanisms of Chromites", in Proceedings Second International Symposium on Solid Oxide Fuel Cells. F. Grosz, P. Zegers, S.C. Singhal and O. Yamamoto, Eds. EUR 13564. Athens Greece. Commission of the European Communities, Luxembourg (1991) 621.

5. N Sakai, T Kawada, H Yokokawa, and M Dokiya. "Thermal Expansion of Some Chromium Deficient Lanthanum Chromites", Solid State Ionics 40/41 (1990) 394.

6. M Mori, N Sakai, T Kawada, H Yokokawa, and M Dokiya. "Low-Temperature Air-Sinterable Lanthanum Calcium Chromite with Chromium Deficit for SOFC Separator", Denki Kagaku 59(4) (1991), 314.

7. WD Kingery and M Berg. "Study of the Initial Stages of Sintering Solids by Viscous Flow, Evaporation-Condensation, and Self-Diffusion", J. Appl. Phys. 26(1955) 1205.

DATE
FILMED
10/8/92